Research paper

DsbA-L ameliorates high glucose induced tubular damage through maintaining MAM integrity

Ming Yang [a,1], Li Zhao [a,b,1], Peng Gao [a], Xuejing Zhu [a], Yachun Han [a], Xianghui Chen [a], Li Li [a], Ying Xiao [a], Ling Wei [a], Chenrui Li [a], Li Xiao [a], Shuguang Yuan [a], Fuyou Liu [a], Lily Q. Dong [c], Yashpal S. Kanwar [d], Lin Sun [a,*]

[a] Department of Nephrology, The Second Xiangya Hospital, Central South University, Changsha, Hunan 410011, China
[b] Department of Pulmonary and Critical Care Medicine, The Second Xiangya Hospital, Central South University, Changsha, Hunan 410011, China
[c] Department of Cell Systems & Anatomy, University of Texas Health at San Antonio, San Antonio, TX 78229, USA
[d] Departments of Pathology & Medicine, Northwestern University, Chicago, IL, USA

ARTICLE INFO

ABSTRACT

Background: The mitochondrial associated endoplasmic reticulum (ER) membrane (MAM) provides a platform for communication between the mitochondria and ER, and it plays a vital role in many biological functions. Disulphide-bond A oxidoreductase-like protein (DsbA-L), expressed in the MAM, serves as an antioxidant and reduces ER stress. However, the role of DsbA-L and MAM in kidney pathobiology remains unclear.
Methods: Molecular biology techniques, transmission electron microscopy (TEM), in situ proximity ligation assays (PLAs), confocal microscopy, TUNEL staining and flow cytometry were utilized to analyse apoptosis and status of MAM in DsbA-L mutant mice.
Findings: We showed that MAM was significantly reduced in the kidneys of streptozotocin-induced diabetic mice, which correlated with the extent of renal injury. We also observed a correlation between the loss of MAM integrity and increased apoptosis and renal injury in diabetic nephropathy (DN). These alterations were further exacerbated in diabetic DsbA-L gene-deficient mice (DsbA-L$^{-/-}$). In vitro, overexpression of DsbA-L in HK-2 cells restored MAM integrity and reduced apoptosis induced by high-glucose ambience. These beneficial effects were partially blocked by overexpression of FATE-1, a MAM uncoupling protein. Finally, the expression of DsbA-L was positively correlated with MAM integrity in the kidneys of DN patients but negatively correlated with apoptosis and renal injury.
Interpretation: Our results indicate that DsbA-L exerts an antiapoptotic effect by maintaining MAM integrity, which is apparently disrupted in DN.

1. Introduction

Diabetic nephropathy (DN) is a serious microvascular complication of diabetes and is the leading cause of end-stage renal disease (ESRD) [1]. Over the last few decades, extensive efforts have been made to elucidate the pathogenesis of DN. In this regard, certain mechanisms have been identified, while others remain to be explored. Recent studies have demonstrated that relentless metabolic perturbations play a critical role in the pathogenesis of DN, which alters cell signalling and disrupts the cell cycle; these changes can be associated with apoptosis, which subsequently leads to tubular damage in DN [2]. Conceivably, these cellular perturbations can alter the behaviour of surviving renal cells associated with increased synthesis of extracellular matrix (ECM), eventually leading to hallmark changes in renal tissues of DN. The hallmarks include thickening of the glomerular and tubular basement membranes and accumulation of ECM in the mesangium and tubulointerstitium, ultimately resulting in glomerulosclerosis and tubulointerstitial fibrosis [3].

In recent years, the biology of ER stress and mitochondrial dysfunction in the pathogenesis of DN has drawn the attention of many investigators. ER stress and mitochondrial dysfunction can trigger apoptosis [4]. Emerging evidence has shown that there are interactions between the mitochondria and ER at their interface, a region known as the mitochondrial-associated ER membrane (MAM) [5,6]. This specialized

* Corresponding author at: Department of Nephrology, The Second Xiangya Hospital, Hunan Key Laboratory of Kidney Disease and Blood Purification, Central South University, No. 139 Renmin Middle Road, Changsha, Hunan 410011, China.
E-mail address: sunlin@csu.edu.cn (L. Sun).
[1] M.Y. and L.Z. contributed equally to this work.

Research in context

Evidence before this study

Excessive apoptosis plays a key role in the development of diabetic nephropathy (DN), but the mechanisms are poorly understood. The mitochondrial-associated endoplasmic reticulum (ER) membrane (MAM) is involved in apoptosis and other biological processes. However, the role of MAM in kidney diseases is unclear. In addition, disulphide-bond A oxidoreductase-like protein (DsbA-L) has been found in MAM proteins by proteomics analysis, but whether it plays a key role in MAM modulation of apoptosis in the diabetic kidney is unclear.

Added value of this study

The expression of DsbA-L is decreased in the kidneys of humans and diabetic mice with DN in association with the uncoupling of MAM integrity; DsbA-L regulates apoptosis of tubular epithelial cells through mitofusin 2 (MFN-2) by maintaining MAM integrity. This change was confirmed for the first time in a renal biopsy of DN patients together with clinical manifestations, such as renal apoptosis and tubular injury.

Implications of all the available evidence

The results provide a novel method for targeting MAM and suggest that DsbA-L may be a potential treatment strategy to alleviate the development of DN.

interface between the mitochondria and ER modulates cellular apoptosis, lipid transport and mitochondrial quality control, among other processes [7]. MAM integrity plays an important role in transferring lipids and in maintaining intracellular homeostasis [7]. Compromised MAM integrity or dysfunction contributes to apoptosis, autophagy and insulin resistance and adversely affects hepatic and skeletal muscle biology [8–12]. The relationship between the morphological changes in MAM integrity and DN, however, remains elusive, especially with respect to its effect on apoptosis of the tubular epithelium, which at times undergoes apoptosis. At times, these changes can be associated with tubulointerstitial injury, especially on a long-term basis, where it would lead to increased ECM synthesis by interstitial cells and thereby fibrosis.

Disulphide-bond A oxidoreductase-like protein (DsbA-L) is a 25-kDa antioxidant enzyme known as glutathione S-transferase (GST)-kappa 1. This enzyme was originally discovered in the mitochondrial matrix [13]. Liu et al. [14] demonstrated that overexpression of DsbA-L can alleviate ER stress and insulin resistance. However, decreased expression of DsbA-L may induce hypertrophic cardiomyopathy [15]. In addition, thickening of the glomerular basement membrane and microalbuminuria have been observed in DsbA-L knockout mice [16]. Moreover, a recent report showed that DsbA-L is found in the MAM proteins via proteomics analysis [17]. However, the role of DsbA-L relative to MAM pathobiology and tubulointerstitial injury in the kidney in DN remains to be fully explored.

Given the above findings, DsbA-L may participate in the modulation of tubular cell apoptosis in the kidney in DN and may cause tubulointerstitial injury in the form of fibrosis on a long-term basis. In the current study, we noted that with perturbation in MAM integrity, the expression of DsbA-L decreased, while it was associated with increased apoptosis in DN mice. In addition, we noted a good correlation between the expression of DsbA-L and altered MAM and apoptosis in diabetic model systems in vivo and in vitro. Additionally, we observed

that altered tubulointerstitial biology was associated with the above indicated perturbations.

2. Materials and methods

2.1. Animal models

A diabetic state was induced in 8-week-old C57BL/6 mice by an intraperitoneal injection of streptozotocin (STZ) (Sigma-Aldrich) in citrate buffer, pH 4.5 (50 mg/kg body weight/day), for five consecutive days [18]. One week following the last injection, the mice with blood glucose levels >200 mg/L were considered diabetic and used for various studies. Mice were euthanized two months after the establishment of a diabetic state. Blood, urine and kidney samples were saved for various biochemical and morphological studies. In addition, DsbA-L$^{+/-}$ mice were obtained from Shanghai Bioray Laboratory, Inc., China (Gene ID, 76263). According to the vendor, the mice were generated on a C57BL/6 background by employing CRISPR/Cas-9 gene-targeting technology. We generated DsbA-L$^{-/-}$ mice by mating male and female DsbA-L$^{+/-}$ mice. Genotyping was performed using a Mouse Direct PCR kit [16]. The primer sequences were as follows: forward primer (5′-GTACACTGGAGTAAGCATTCTGGTATC-3′); reverse primer (5′-CTTG ATATCCTATGAAAGCCTCAGC-3′). Gene disruption of the DsbA-L gene was also confirmed by nucleotide sequencing. The DsbA-L$^{-/-}$ littermate wild-type mice were used as the control group. All mice were housed at 22-26 °C in a quiet room in animal facilities with a 12-hr light-dark cycle. The animals were divided into four groups: control littermates (C57BL/6J), STZ-induced diabetic mice, DsbA-L$^{-/-}$ mice and DsbA-L$^{-/-}$ with STZ-induced diabetic mice (n = 8). All animal experiments were performed in accordance with the regulations established by the Institutional Committee for Care and Use of Laboratory Animals at Central South University, China.

2.2. Assessment of physiological features and renal function

Every two weeks, mouse body weight was measured, and urine and blood samples were collected. Blood glucose levels were determined by a blood glucose monitor (Boehringer Mannheim, Germany). Urine albumin was measured by enzyme-linked immunosorbent assay (ELISA; Bethyl Laboratories, USA). Urine creatinine concentrations were determined using an ELISA kit (Exocell, Philadelphia, USA). Urinary ACR was calculated as the urine albumin/creatinine ratio.

2.3. Renal histology and immunohistochemistry (IHC)

Morphological changes were assessed in kidney tissue sections stained with haematoxylin and eosin (HE), periodic acid Schiff (PAS) and Masson's trichrome. A semiquantitative scoring system was used to evaluate the degree of tubulointerstitial injury. Paraffin-embedded kidney sections were also used for IHC studies. The kidney tissue sections were dewaxed, rehydrated, subjected to antigen retrieval and individually incubated with the following antibodies: anti-DsbA-L polyclonal antibody (Proteintech, 1:200), anti-MFN-2 polyclonal antibody (Proteintech, 1:200) and anti-cleaved caspase-3 polyclonal antibody (CST, 1:200). After an overnight incubation at 4 °C, the samples were incubated with secondary antibodies for 1 h at 22 °C, treated with diaminobenzidine, and counterstained with haematoxylin. The sections were examined by light microscopy.

2.4. In situ proximity ligation assay (PLA)

The status of the MAM was evaluated using an in situ PLA (Olink Bioscience), which enables the detection, exteriorization, and quantification of MAM interactions as previously described [10]. Briefly, paraffin-embedded kidney sections were dewaxed, rehydrated, subjected to antigen retrieval and successively incubated with an

anti-voltage-dependent anion channel 1 (VDAC1) polyclonal antibody (Proteintech, 1:200) and then anti-IP3R1 polyclonal antibody (Proteintech, 1:200) overnight at 4 °C. The sections were then incubated with the PLA probe for 1 h, followed by ligation and amplification in the presence of polymerase. The relative MAM integrity was evaluated by ImageJ software, and the IP3R1-VDAC1 dots were quantified and are expressed as the percentage of dots per nucleus, as described previously [10,11,20].
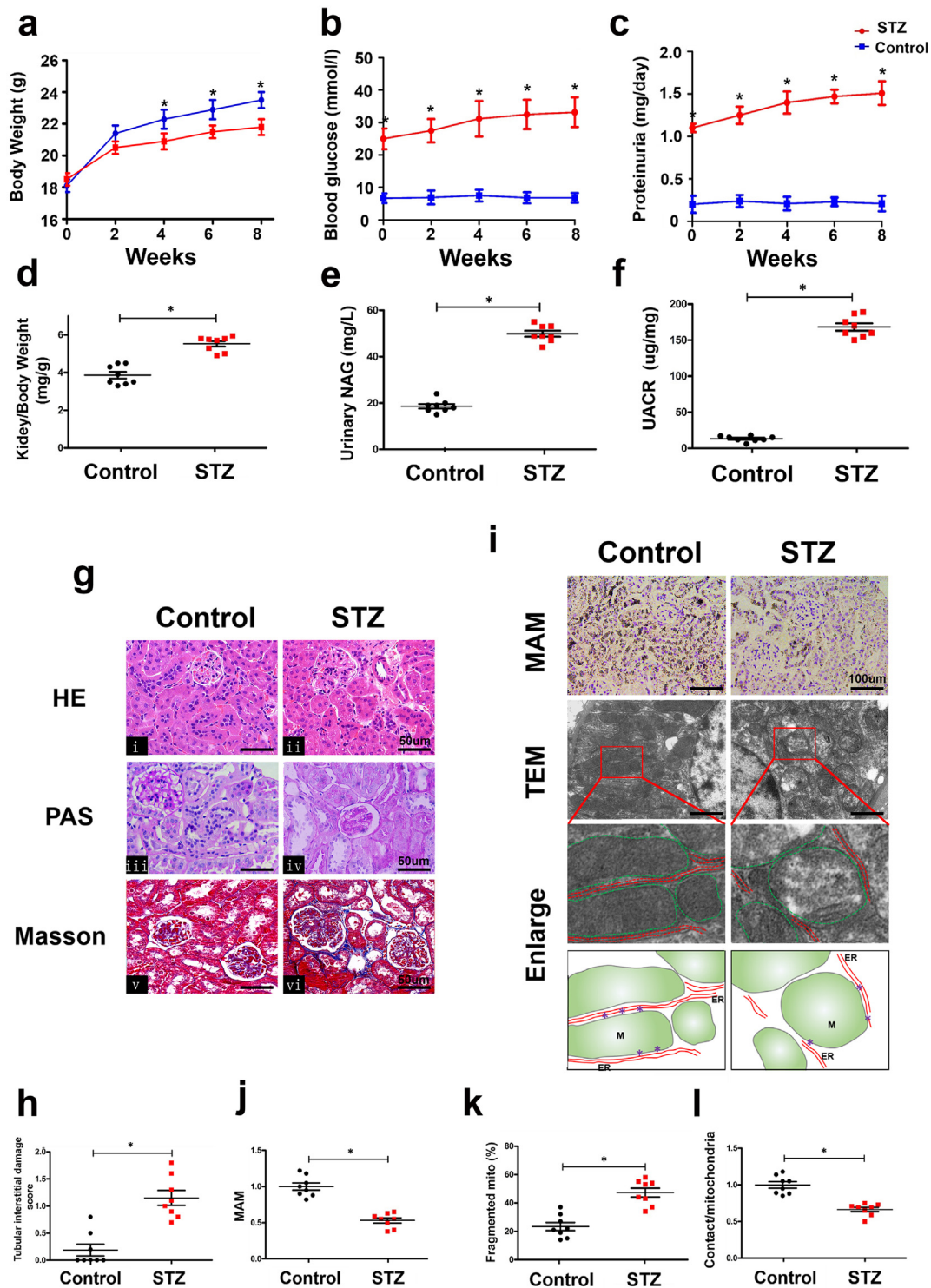

Fig. 1. Pathological changes and disruption of mitochondrial-associated endoplasmic reticulum membrane (MAM) coupling in the kidneys of STZ-induced diabetic mice. Compared with the control mice, streptozotocin (STZ)-induced diabetic mice had a decreased body weight (a) and significantly increased blood glucose (b), proteinuria (c), kidney/body weight (d), urinary NAG (e) and UACR (f). Renal pathological changes were detected by HE, PAS, and Masson staining (g). h: Represents the degree of tubular injury in DN as assessed by the tubular interstitial damage score, which was higher in DN mice than control mice. By the in situ proximity ligation assay (PLA), a notably reduced number of MAMs was observed in the kidneys of DN mice compared with the controls (i, top panels and j). An electron microscopic image showing fragmented mitochondria in tubular cells and a significant drop in mitochondrial-ER coupling compared with those of the control group (i. second and third panels, k & l). (i, lower panel) Tracing of the mitochondria and ER from the aforementioned TEM micrographs. Data was showed as mean ± SD. n = 8, *p < 0.05 indicates a significant difference compared with the control.
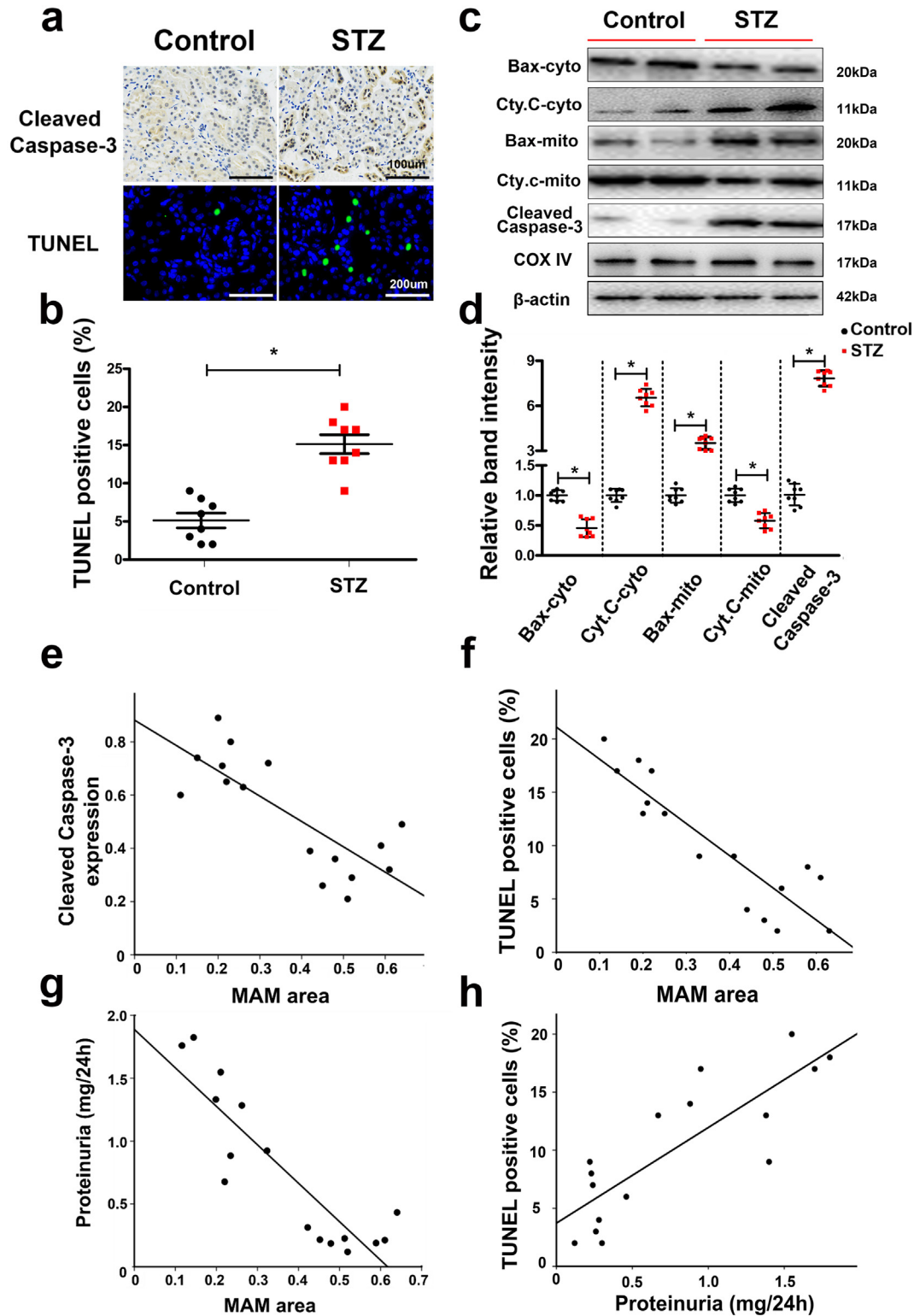
Fig. 2. Apoptosis of renal tissues was closely related to MAM integrity in the kidneys of diabetic mice. By immunohistochemistry (IHC) with an anti-cleaved-caspase-3 antibody (a, upper panels) and TUNEL staining (a, lower panels and b), the number of apoptotic tubular cells in the kidneys of diabetic mice was shown to be notably increased compared with that of the control. c: Western blot analysis showing Bax and Cyto. C expression in the cytoplasm from the kidney (c, first and second lines), Bax and Cyto. C expression in mitochondria extracted from the mouse kidney (third and fourth lines) and cleaved caspase-3 expression in total protein from the kidney (fifth lines). No change was observed in COX IV and β-actin expression in the mitochondria and total protein from the kidney (sixth and seventh lines). Scatter diagram representing the relative band intensity results from Western blot analysis (d). Correlation analysis between the MAM area from in situ PLA and cleaved caspase-3, $r = -0.769$ ($p < 0.05$) (e), MAM and number of TUNEL-positive cells, $r = -0.793$ ($p < 0.05$) (f), MAM and proteinuria, $r = -0.743$ ($p < 0.05$) (g), and proteinuria and the number of TUNEL-positive cells, $r = 0.681$ ($p < 0.05$) (h). Cyt. C, Cytochrome C; cyto, cytosol; mito, mitochondrial; r: correlation coefficient; values are the mean $\pm$ SE. n = 8. *$p < 0.05$ compared with the control group.
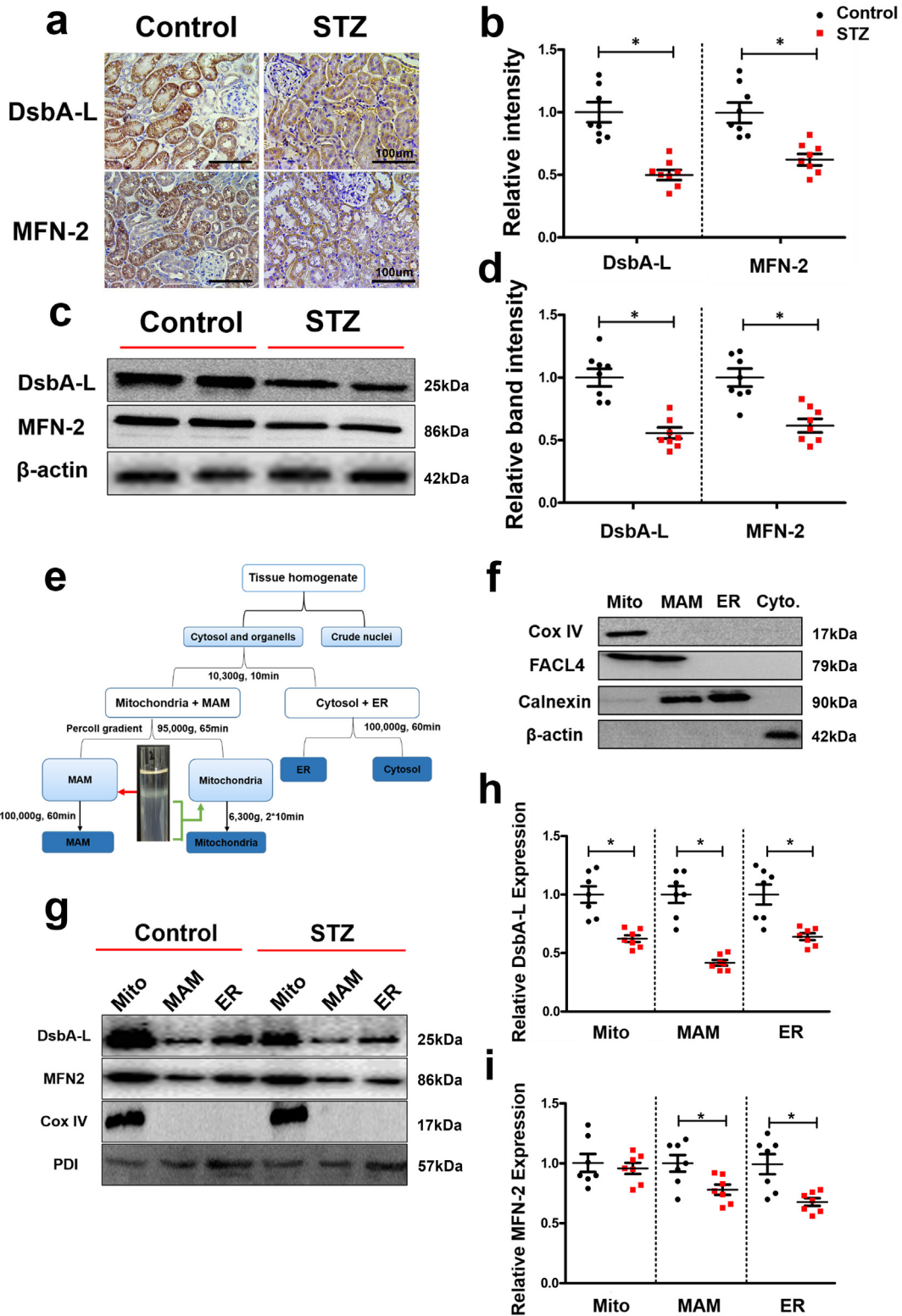
Fig. 3. Identification of DsbA-L as an MAM protein and significantly reduced expression of DsbA-L and MFN2 in the kidneys of diabetic mice. IHC staining showing that the protein expression levels of DsbA-L and MFN-2 were notably reduced in the DN mouse kidney (a and b). c: Western blot analysis. d: Scatter diagram representing the related band intensity results of the Western blot analysis. e: The protocol for isolation of the MAM proteins from mouse kidney. f. Western blot analysis of the purity of the MAM-related proteins. g: Western blot analysis of DsbA-L and MFN2 expression in the mitochondria, MAM and ER. h-i: Representative relative band intensity by Western blot analysis. Values are the mean ± SE. n = 8. *p < 0.05 compared with the control group. Mito: crude mitochondria; MAM: mitochondrial associated ER membrane; ER: endoplasmic reticulum.
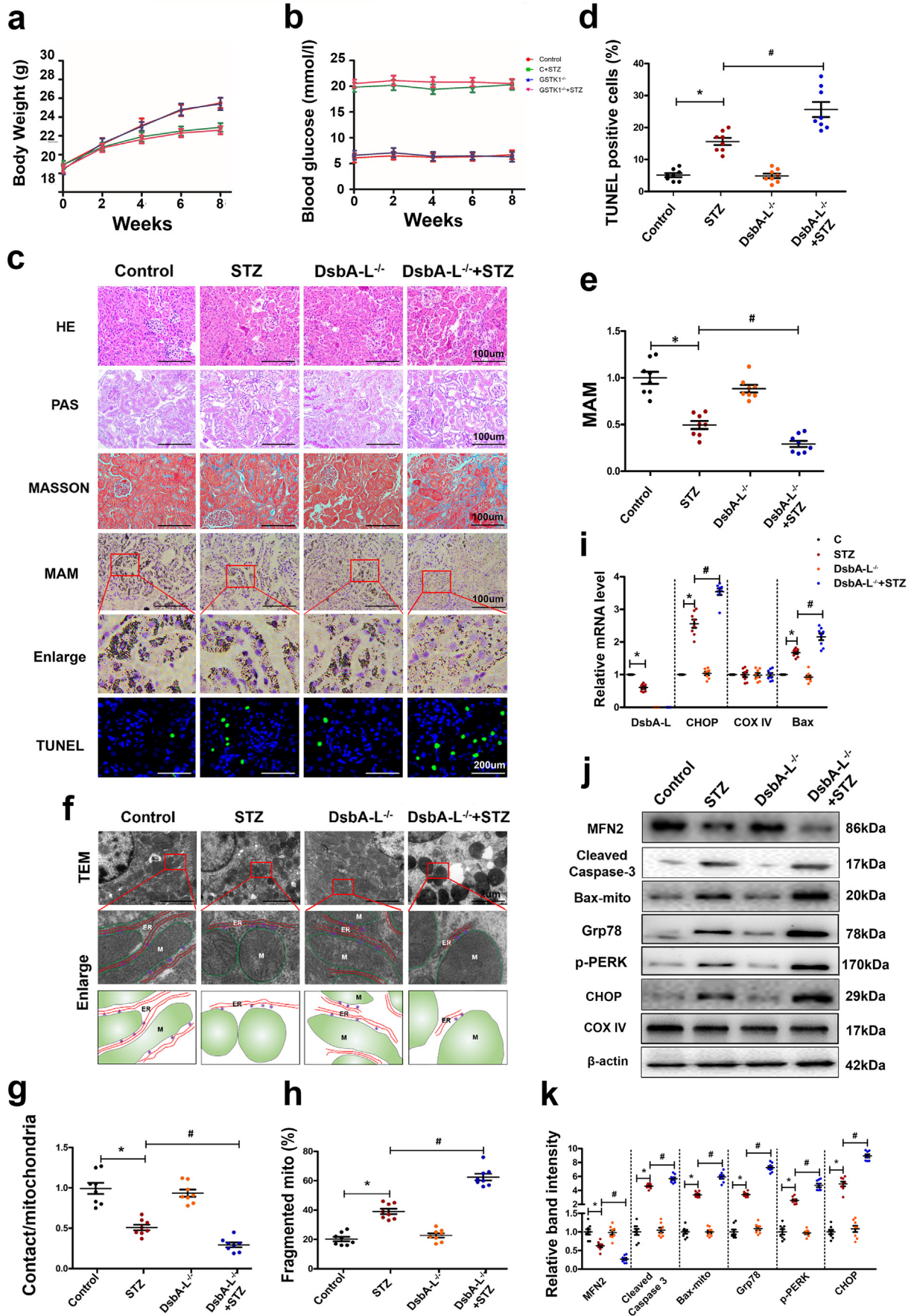
Table 1
The activities of phospholipid biosynthetic enzymes in MAMs from mouse kidney from different groups.

	Control	STZ	DsbA-L$^{-/-}$	DsbA-L$^{-/-}$ + STZ
PtdSer synthase (nmol/min/mg protein)	17.8 ± 3.6	10.5 ± 2.5*	16.6 ± 4.2	7.3 ± 1.1[#]
PtdEtn methyltransferase (nmol/min/mg protein)	2.43 ± 0.37	1.32 ± 0.24*	2.44 ± 0.29	0.75 ± 0.38[#]

PtdSer: phosphatidylserine; PtdEtn: phosphatidylethanolamine. Data are the mean ± SD of MAMs from different groups. n = 8.
* p < 0.05 compared with the control group.
# p < 0.05 compared with the STZ group.

2.5. Assessment of the MAM integrity by transmission electron microscopic analysis

The mitochondrial morphology and ER-mitochondrial contacts were assessed by transmission electron microscopy (TEM). The extent of fragmented mitochondria and MAM contact points in ultrathin sections were assessed using ImageJ software. The percentage of mitochondria membrane in contact with ER within a 50 nm range was measured and normalized to mitochondria perimeter, as previously reported [10,21].

2.6. MAM purification and functional analysis

The MAM, mitochondria, and ER membranes were isolated from the kidney and cells by Percoll gradient fractionation. Briefly, 100 mg of kidney tissues or HK-2 cells from ten 10 cm dishes was harvested at 4 °C in a phosphate buffer solution (PBS). The samples were lysed in a Dounce homogenizer in buffer 1 (sucrose homogenization medium, 0.25 M sucrose, 10 mM HEPES, pH 7.4) supplemented with protease inhibitors. The homogenate was centrifuged at 600 ×g for 5 min twice to collect the supernatant. The supernatant was re-centrifuged 3 times for 10 min at 10,300 ×g. The resulting pellet (crude mitochondrial fraction) and supernatant (ER fraction) were saved. The crude mitochondrial fraction was layered on a 30% Percoll gradient in buffer 2 (0.225 M mannitol, 5 mM HEPES, 0.5 mM EGTA, pH 7.4) and centrifuged at 95,000 ×g for 65 min using a Beckman ultracentrifuge in a 41.1 SW rotor. The pure mitochondrial fraction was obtained at the bottom of the tube, and MAMs were localized to the intermediate layer. The MAM fraction was centrifuged at 100,000 ×g for an additional 60 min, whereas the mitochondrial fraction was centrifuged twice at 6300 ×g for 10 min. The ER fraction was harvested following centrifugation of the intermediate layer at 100,000 ×g for 60 min. All pellets were resuspended in 2 mL buffer 2, as previously described [22]. The protein concentration was determined using the Bicinchoninic Acid (BCA) Assay kit from Beyotime Biotechnology. Equal amounts of protein (25 μg) from each fraction were fractionated by sodium dodecyl sulphate polyacrylamide gel electrophoresis (SDS-PAGE), and immunoblotting analysis was performed.

The function of MAMs isolated from the mouse kidneys of various groups was assessed by detecting the activities of phospholipid biosynthetic enzymes as described previously [23].

2.7. Cell culture and stably transfected cell lines

The human proximal tubular epithelial cell line (HK-2 cells) was purchased from ATCC (USA) and maintained in medium containing 5 or 30 mM D-glucose in 5% CO$_2$ and 95% air at 37 °C. For overexpression of DsbA-L, PcDNA3.1- DsbA-L plasmid (gift from Dr. Feng Liu [24]) was transfected into HK-2 cells using Lipofectamine 2000 (Invitrogen, Carlsbad, CA), and stable transfectants were selected in the presence

of 800 μg/mL G418 in the medium. The PcDNA4-FATE-1 (Fetal And Adult Testis Expressed-1) plasmid (gift from Dr. Jennifer Rieusset [10]) was subcloned into PcDNA3.1, and the recombinant plasmid was transfected into HK-2 cells with stable overexpression of DsbA-L transfectants. HK-2 cells that overexpressed DsbA-L-FATE-1 were characterized by Western blot analysis.

2.8. Assessment of apoptosis by flow cytometry

After treatment with various interventions, cells were collected and then incubated with Annexin V-fluorescein isothiocyanate (FITC) (Santa Cruz Biotechnology) and propidium iodide (PI), as described previously [25]. Data were analysed by using a fluorescence activated cell sorting (FACS) Calibur system (BD Biosciences).

2.9. Analysis of apoptosis

Terminal deoxynucleotidyl transferase dUTP nick end-labelling (TUNEL) staining was used to detect apoptosis according to the manufacturer's instructions [26,27].

2.10. Quantitative real-time PCR

Kidney tissues and HK-2 cell RNA were extracted and then reverse-transcribed into cDNA using a TaKaRa cDNA Synthesis Kit. SYBR premix EXTaqTM reagents were used to perform real-time PCR [28]. The data are presented as fold changes ($2^{-\Delta\Delta Ct}$).

2.11. Assessment of the MAM in vitro by immunofluorescence

The MAM status was also assessed by immunofluorescence, as previously described [29,30]. Briefly, HK-2 cells were stained with MitoTracker and ER-Tracker dyes. The cells were counterstained with 4′,6-diamidino-2-phenylindole (DAPI) to visualize the nuclei. The cells were examined by confocal microscopy.

2.12. Human kidney

Patients with biopsy-proven DN (n = 10) and cohorts with nondiabetic renal diseases, such as glomerular minor lesion (GML) (n = 10), were used as controls [27,31]. The renal biopsy tissues were subjected to H&E, PAS, PASM, and TUNEL staining, as well as in situ PLA, as described above. Tubulointerstitial injury indices were assessed by a semiquantitative scoring system, as described previously [26].

2.13. Study approval

This study protocol was approved by the medical ethics committee of The Second Xiangya Hospital, central south university

Fig. 4. Disruption of MAM integrity and increased apoptosis in the kidneys of DsbA-L gene-deficient mice. Body weight (a), blood glucose (b). The kidney sections were stained with HE, PAS, Masson, TUNEL and in situ PLA (c). Scatter diagram representing the levels of TUNEL-positive cells (d) and the MAM integrity (e). Electron microscope image showing MAM coupling in the kidney and fragmented mitochondria and the tracing of mitochondria and ER from the aforementioned TEM micrographs (f, g & h). i: mRNA analysis of DsbA-L, CHOP, COX IV and bax. j: Western blot analysis of the expression of Bax, cleaved-caspase-3, MFN-2, Grp78, p-PERK and CHOP in kidneys. k: Scatter diagram representing the relative band intensity by Western blot analysis. Values are the mean ± SE. n = 8. *p < 0.05 compared with the control group; #p < 0.05 compared with the DN group.
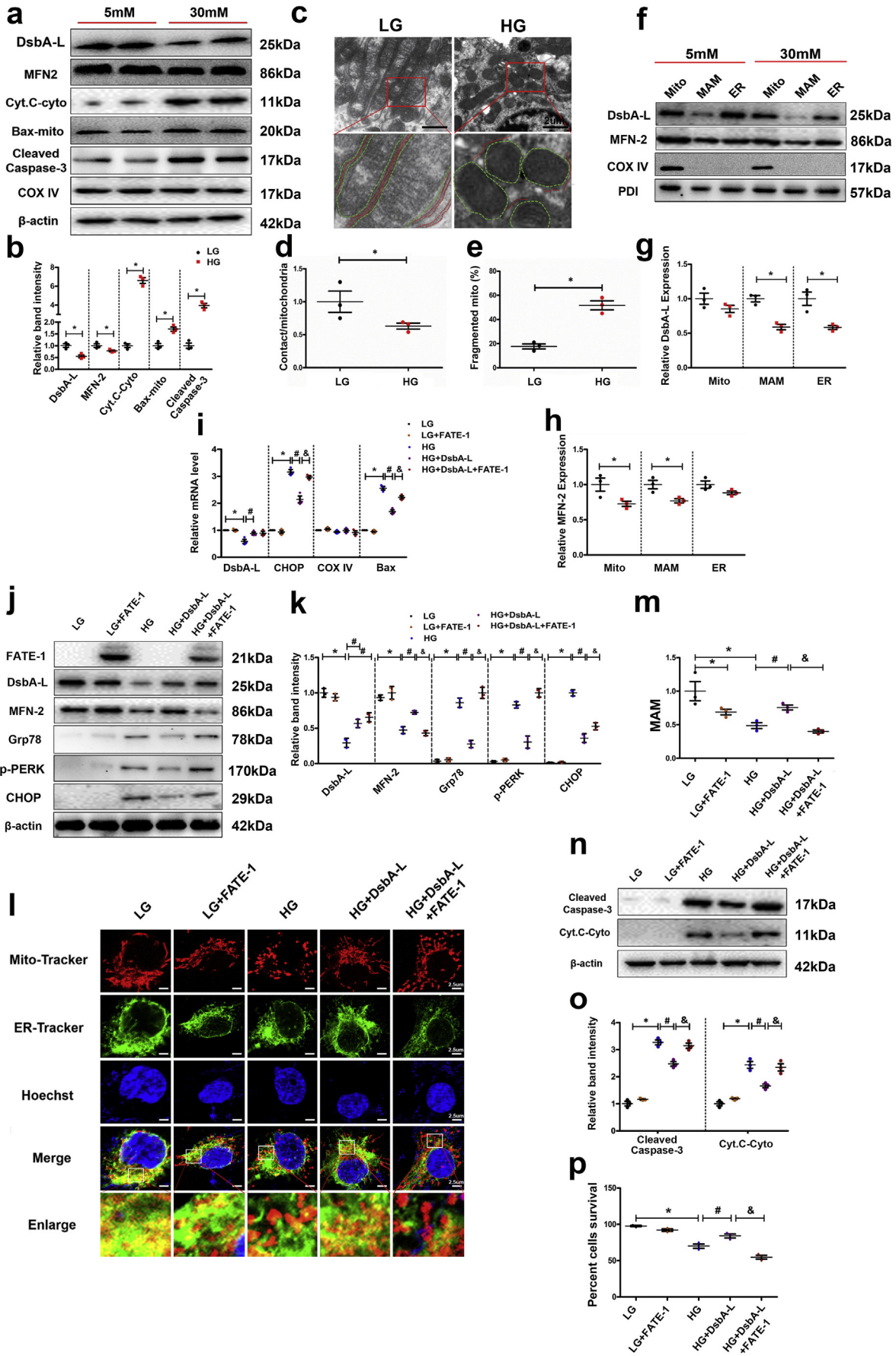
(No. 2017-S112). All the patients gave informed consent for participating in this study.

2.14. Statistical analysis

All statistical analyses were performed using SPSS 20.0 software. The results are expressed as mean $\pm$ standard deviation ($\pm SD$) and were assessed by one-way analysis of variance (ANOVA). Correlations between two numerical variables were tested by correlation analysis. A value of $p < 0.05$ was considered as the significant difference between groups.

3. Results

3.1. Pathological alterations in mice with STZ-induced diabetes

A significantly reduced body weight and higher blood glucose levels, proteinuria, kidney/body weight, urinary NAG and UACR were observed in STZ-induced mice compared to control mice (Fig. 1a-f). H&E staining showed minimal changes in the glomerular morphology in kidneys from STZ-induced DN mice (Fig. 1g i & ii). Therefore, we focused on the changes in the mitochondria enriched tubular compartment. PAS and Masson staining showed notably increased tubular brush border staining and tubulointerstitial fibrosis in the kidneys of diabetic mice compared to controls (Fig. 1g iii-vi). Visual quantification revealed significant tubulointerstitial damage in DN mice compared to the controls (Fig. 1h). In addition, to quantify the integrity of the MAM in paraffin sections of kidney tissue, we performed in situ PLA with the use of VDAC1 and IP3R1 antibodies. The MAM-associated staining was notably decreased in tubular cells of the kidney in diabetic mice compared with the controls (Fig. 1i & j). Electron microscopy revealed that the fragmented mitochondria were significantly increased in renal tubular cells of diabetic mice (Fig. 1i & k), which was accompanied by a loss of MAM contact points localized at the interface of the ER and outer mitochondrial membrane (Fig. 1i & l).

3.2. Relevance of apoptosis to MAM integrity in the renal tubules of DN mice

IHC staining showed that the expression of cleaved caspase-3, a widely acknowledged executioner of the apoptotic pathway, was notably increased in the kidneys of STZ-induced diabetic mice compared to the controls (Fig. 2a, upper panels). This change was accompanied by an increased degree of apoptosis in renal tubular epithelial cells, as indicated by TUNEL staining (Fig. 2a, lower panels and 2b). Western blot analysis revealed significantly decreased expression of Bax in the cytoplasmic fraction of renal cells of diabetic mice, while it was increased in the mitochondrial fraction (Fig. 2c & d). Very low expression of cleaved caspase-3 was observed in the kidneys of control animals, but it was markedly increased in diabetic mice (Fig. 2c & d). No significant changes were observed in the renal expression of COX IV and β-actin, which served as loading controls (Fig. 2c). Correlation analyses revealed a negative correlation between the MAM integrity (which was detected by in situ PLA) and expression of cleaved caspase-3 from IHC ($r = -0.769$, $p < 0.05$) (Fig. 2e), TUNEL- positive cells ($r = -0.793$, $p < 0.05$) (Fig. 2f) and proteinuria ($r = -0.743$, $p < 0.05$) (Fig. 2g). However, a marked strong positive correlation was noted

between proteinuria and TUNEL-positive cells ($r = 0.681$, $p < 0.05$) (Fig. 2h).

3.3. Expression of DsbA-L and mitofusion-2 (MFN2) is downregulated in mitochondria and MAM isolated from the kidneys of diabetic mice

By IHC, the expression of DsbA-L was downregulated in the tubules of STZ-induced diabetic mice with concomitant reduced expression of MFN-2, a protein that determines the shape and structural morphology of the mitochondria (Fig. 3a & b). Similar results were observed in Western blot analysis, where decreased expression of both proteins was noted (Fig. 3c & d). To determine whether DsbA-L was expressed in the MAM area, we homogenized the mouse kidney and fractioned it into the mitochondria, MAM, ER and cytoplasm fractions, as shown in Fig. 3e. The purified MAM was identified by Western blot analysis with various antibodies, as described previously [22]. As shown in Fig. 3f, cytochrome C oxidase subunit IV (COX IV), an inner membrane protein of the mitochondria, was only expressed in mitochondria, while fatty acid-CoA ligase 4 (FACL4) was expressed in mitochondria and MAM, and calnexin was expressed in the MAM and ER. These observations are consistent with previous literature reports, meaning that MAM isolated from the kidney was satisfactorily purified for further use [7]. Furthermore, the expression of the DsbA-L and MFN-2 proteins was observed in isolated mitochondria, the MAM and the ER, but the expression levels of DsbA-L in the MAM, mitochondria, and ER extracted from the kidneys of diabetic mice were significantly downregulated compared with those of the control (Fig. 3g panel 1, lines 1 vs 4, 2 vs 5, and 3 vs 6. Fig. 3h). Similarly, the expression of MFN-2 in the MAM and the ER was decreased (Fig. 3g panel 2 lines 2 vs 5 and 3 vs 6. Fig. 3i). There were no significant changes in the expression of COX IV expression in the mitochondrial fraction (Fig. 3g panel 3). Likewise, there were no differences in the expression of protein disulphide isomerase (PDI) in the mitochondria, MAM and the ER fractions between the DN and control mice (Fig. 3g panel 4).

3.4. Pathophysiologic perturbations in diabetic DsbA-L gene-deficient mice, MAM integrity (contacts at the interface of ER and mitochondria) and function and proteins relevant to apoptosis

Higher blood glucose levels and lower body weights were noted in STZ-induced diabetic C57BL/6J mice compared to control mice (Fig. 4a & b). The degree of change in body weight and blood glucose levels was relatively high in diabetic DsbA-L$^{-/-}$ mice (Fig. 4a & b). Along these lines, the diabetic DsbA-L$^{-/-}$ mice showed relatively severe tubular epithelial changes and increased interstitial fibrosis (Fig. 4c). The changes were readily observed in PAS-stained sections and were reflected by the relative loss of epithelial cell integrity, brush borders and widening of the interstitial space. The latter may be due to increased ECM synthesis by the surviving interstitial cells. The changes were not obviously discernible in the glomerular compartment. Likewise, the highest degree of apoptosis was observed in diabetic DsbA-L$-/-$ mice compared to C57BL/6J diabetic mice or controls (Fig. 4c & d). Interestingly, in situ PLA staining revealed markedly decreased ER-mitochondria interactions in the kidneys of diabetic DsbA-L$^{-/-}$ mice compared with that of diabetic C57BL/6J or control mice (Fig. 4c & e). In addition, the activities of phospholipid biosynthetic enzymes were decreased significantly in MAMs from the kidneys of diabetic mice

Fig. 5. Expression of DsbA-L, MFN-2, Cyt. C, Bax and caspase-3 as well as the altered MAM integrity in HK-2 cells. (a) After HG treatment for 24 h, Western blot analysis showing DsbA-L, MFN-2, Bax, and cleaved caspase-3 expression in total protein from HK-2 cells (first, second and fifth lines), Cyt. C expression in the cytoplasm of HK-2 cells (third line), and Bax expression in mitochondria extracted from HK-2 cells (fourth line) was performed. Relative band intensity of the Western blot analysis shown in b. TEM analysis of HK-2 cells in LG and HG (c, d and e). Western blot analysis of DsbA-L and MFN2 expression in the mitochondria, MAM and ER (f). g-h: Representative relative band intensity by Western blot analysis. i: mRNA analysis of DsbA-L, CHOP, COX IV and bax. Western blot analysis of the expression of FATE-1, DsbA-L, MFN-2, Grp78, p-PERK and CHOP (j). k: Scatter diagram representing the related band intensity. Confocal image with MitoTracker and ER-Tracker staining showing the MAM integrity in HK-2 cells (l) and quantitative analysis by a scatter histogram (m). n: Western blot analysis of the expression of cleaved caspase-3 in total protein (first line) and Cyt. C in the cytoplasm (second line). o: Representative related band intensity by Western blot analysis. p: Quantification of FACS analyses of five experiments. Values are the mean $\pm$ SE. $n = 3$. *$p < 0.05$ compared with the control, #$p < 0.05$ compared with HG, &$p < 0.05$ compared with HG with DsbA-L overexpression.
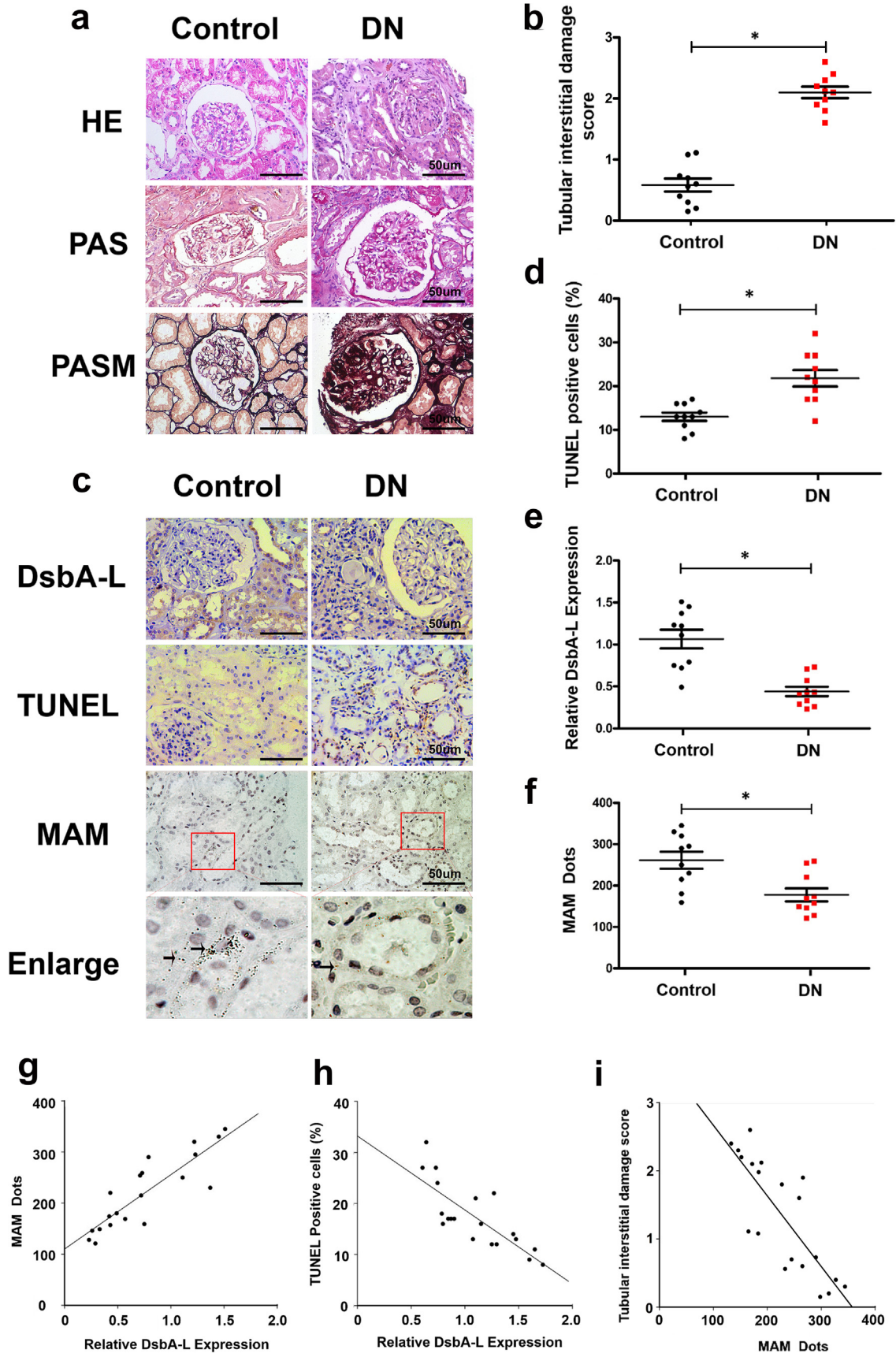
compared to controls, while they were further aggravated in those of diabetic mice deficient in the DsbA-L$^{-/-}$ gene (Table 1). By TEM, a notable increase in the fragmented mitochondria and a decrease in the MAM integrity were observed in the kidneys of diabetic DsbA-L$^{-/-}$ mice compared with those of C57BL/6J diabetic mice (Fig. 4f, g & h). However, the mRNA level of the apoptotic protein Bax was notably increased in diabetic mice compared to control mice, while it was further increased in diabetic DsbA-L$^{-/-}$ mice. Similar results were observed for the CHOP (C/EBP homologous protein) gene, an ER stress marker, and no change was observed in the expression of the COX IV gene (Fig. 4i). Western blotting analysis revealed substantially decreased expression of MFN2 in the kidneys of DsbA-L$^{-/-}$ diabetic mice compared to those of the controls (Fig. 4j & k). In contrast, the protein expression of cleaved caspase-3, bax-mito and ER stress related proteins such as GRP78 (glucose 2 regulated protein 78 kD), p-PERK (phospho-protein kinase RNA-like endoplasmic reticulum kinase) and CHOP were increased significantly in the kidney of diabetic mice compared to the control, while it was further aggravated in DsbA-L−/− diabetic mice (Fig. 4j & k).

3.5. Effect of high glucose (HG) conditions on the expression of DsbA-L and mitochondrial, ER and MAM homeostasis in HK-2 cells

In Western blot analysis, the expression of DsbA-L and MFN-2 in HK-2 cells exposed to HG conditions was decreased (Fig. 5a). No discernible changes were observed following treatment with 30 nM mannitol, which served as the osmotic control (data not included). The expression of Cyt. C was significantly increased in the cytoplasmic fraction of HK-2 cells treated with HG (Cyt. C-cyto, Fig. 5a). The expression of Bax was increased in the mitochondrial fraction compared to that of cells treated with low glucose (LG) (Fig. 5a), and the expression of cleaved caspase-3 was also increased in HK-2 cells exposed to HG conditions (Fig. 5a). The relative binding intensity of various immunoblotted proteins is included in Fig. 5b. A notable increase in the fragmented mitochondria and a decrease in the MAM integrity were observed in HK-2 cells treated with HG compared to LG (Fig. 5c, d & e). Interestingly, the expression of DsbA-L in the MAM and ER cellular fractions was decreased in HK-2 cells treated with HG (Fig. 5f & g). Additionally, MFN2 expression was decreased in the mitochondria and the MAM fractions (Fig. 5f & h). The expression of COX IV and PDI was not significantly altered in the mitochondrial, MAM and ER fractions of HK-2 cells treated with LG vs HG (Fig. 5f).

To elucidate the mechanisms by which DsbA-L regulates MAM homeostasis in HK-2 cells, we transfected the cells with the DsbA-L and FATE-1 expression plasmids. As previously reported, the FATE-1 protein is localized in the MAM, and it shows homology with mitochondrial fission factor (MFF) and regulates the distance between the mitochondria and ER. The mRNA levels of Bax and CHOP were notably increased in HK-2 cells treated with HG, while the effect was partially blocked in cells overexpressing DsbA-L, and the effect of DsbA-L overexpression was blocked by transfection of the FATE-1 plasmid (Fig. 5i). In addition, a notable increase was observed in the expression of FATE-1 and DsbA-L in HK-2 cells following transfection of plasmids under LG conditions (Fig. 5j & k). Interestingly, overexpression of DsbA-L led to the restoration of HG-induced changes in MFN-2, Grp78, p-PERK and CHOP expression (Fig. 5j & k), while the effect was partially blocked following cotransfection with the FATE-1 plasmid. For confirmation of the effect of DsbA-L on MAM integrity in HK-2 cells, the cells were exposed to HG conditions and then observed by laser scanning confocal microscopy, afterwards cells were subjected to double staining with MitoTracker Red and ER-Tracker Green [29,30]. The overlapping yellow

Table 2
Characteristics of the renal biopsy tissue for diabetic nephropathy (DN) patients and patients with glomerular minor lesion (GML).

Subjects	n	Gender ratio	Age (years)	BMI (kg/m^2)	HbA1c (%)
DN	10	6 M/4 W	55 ± 2.9	24 ± 2.7*	7.9 ± 0.5*
GML	10	5 M/5 W	52 ± 4.2	20 ± 3.2	4.9 ± 0.6

BMI: body mass index.
* $p < 0.05$ compared with the control group.

staining observed in the overlay images indicates the area of colocalization of the mitochondria and the ER, which basically represents the MAM. Treatment with HG or overexpression of FATE1 in HK-2 cells significantly reduced the MAM interface, while the effect of HG was negated by transfection with the DsbA-L plasmid (Fig. 5l & m). Furthermore, the DsbA-L-restored MAM interface under HG was abolished by cotransfection with the FATE1 plasmid. The overexpression of DsbA-L also reduced the expression of cleaved caspase-3 in HK-2 cells treated with HG (Fig. 5n & o. Interestingly, this beneficial effect was partially blocked following cotransfection with the FATE1 plasmid (line 5 vs 4). Similar results were observed for the cytoplasmic Cyt. C expression patterns in cells undergoing various treatments (Fig. 5n & o). In addition, FACS data showed that HK-2 cells treated with various factors showed a similar trend (Fig. 5p).

3.6. Decreased expression of DsbA-L and altered MAM integrity are associated with kidney injury in patients with DN

A survey of renal biopsies of diabetic patients stained with H&E, PAS and PASM revealed increased mesangial matrix and nodular glomerulosclerosis, indicating that these patients have well-established renal lesions of DN (Fig. 6a). After matching the BMI and age of the patients with DN with the controls (Table 2), we examined the tubulointerstitial compartment (Fig. 6b). IHC staining revealed notably decreased expression of DsbA-L in the renal tubular compartment of DN patients compared with the controls (Fig. 6c & e). Additionally, MAM staining was notably reduced as shown by in situ PLA staining, and it was accompanied by an increased number of apoptotic cells (Fig. 6c, d & f). Correlation analyses revealed a positive correlation between the degree of MAM staining and expression of DsbA-L (r = 0.748, p < 0.05) (Fig. 6g), while a negative correlation was observed between DsbA-L and apoptosis (r = −0.631, p < 0.05) (Fig. 6h). Finally, the MAM staining showed a negative correlation with the degree of tubular damage (r = −0.653, p < 0.05) (Fig. 6i).

4. Discussion

Increased renal apoptosis in patients with DN and tubulointerstitial fibrosis in human DN and animal models were correlated with renal tubular cell injury involving a multitude of signalling mechanisms. Among many events, apoptosis is one of the notable occurrences in DN, and it is believed to play a role in the development of DN [33]. Unfortunately, the detailed mechanisms of these phenomena are unclear and thus requires further investigation. Moreover, there are no available suitable therapeutic agents that can reverse the progress of these pathological changes, which further emphasizes the need to explore additional mechanisms that are relevant to the pathogenesis of DN. In this study, we demonstrated that the DsbA-L/MFN-2 pathway, which modulates MAM functionality, may serve as a therapeutic target in relieving kidney injury in diabetes.

Fig. 6. Altered MAM integrity and DsbA-L expression are associated with tubular damage in the kidneys of patients with DN. (a) HE, PAS, and PASM staining showing the pathological changes in the renal biopsy of DN patients. (b) Representative degree of tubular injury in DN patients. (c) IHC staining with an anti-DsbA-L antibody (panel 1 from upper), TUNEL staining (panel 2 from upper) and in situ PLA (panel 3 and 4 from upper). (d) Scatter diagram representing the level of TUNEL-positive cells, DsbA-L expression (e) and MAM integrity (f). (g) Correlation analysis between DsbA-L expression and MAM dots (r = 0.748, p < 0.05), (h) MAM dots and the number of TUNEL-positive cells (r = −0.631, p < 0.05) and (i) MAM and the tubular interstitial damage score (r = −0.653, p < 0.05). Values are the mean ± SE. n = 10. *p < 0.05 compared with the control group.

The MAM, as an interface between mitochondria and the ER, is a dynamic structure that maintains cellular homeostasis [34]. In addition, the dynamic equilibrium of the MAM is dependent on nutritional requirements. Recent research has shown that distances that are too close (<7 nm) or too wide (>50 nm) between mitochondria and the ER will result in dysfunction of MAMs [35]. In this study, the MAM integrity is shown as the percentage of the mitochondrial membrane in contact with the ER within a 50 nm range and was normalized to the mitochondria perimeter as described previously [10]. With the disruption of MAM integrity, various factors are activated and lead to cellular injury, such as oxidative stress and apoptosis. Previous studies have shown that the tight interactions between mitochondria and the ER promote mitochondrial respiration and bioenergetics [37]. HG conditions can disrupt the MAM integrity and cause mitochondrial fragmentation, which leads to a decrease in mitochondrial respiration in hepatocytes probably through the pentose phosphate-protein phosphatase 2A (PP-PP2A) pathway [38]. Likewise, the MAM integrity has been reported to be significantly compromised in the islets of patients with diabetes [11]. However, other early research has shown that excessive ER-mitochondria coupling can also result in organelle dysfunction and oxidative stress in the liver of *ob/ob* mice and mice with obesity induced by high-fat diet (HFD) administration. Further investigation reported that uncoupling of the MAM can recover the mitochondrial oxidative capacity and glucose metabolism [39]. These contradictory observations may be a consequence of employing different animal models and methods used to study MAM pathobiology. Emerging evidence indicates that in situ PLA is a reliable method to measure the status of MAM in various tissues, such as the liver and skeletal muscle [20,38,42]. However, the status of MAM integrity in the kidney has not been well documented. Here, we analysed the interface between the ER and mitochondria, i.e., MAM, in the kidneys of diabetic patients and animal models using in situ PLA technology. We observed that the MAM integrity was compromised in the renal biopsy tissues of DN patients and the kidneys of mice with STZ-induced diabetes, and our findings were consistent with previous observations made in the liver and skeletal muscle in states of obesity [10,20]. Furthermore, the morphological changes in the MAM were also confirmed by TEM. Interestingly, the change in MAM integrity was associated with increased apoptosis in tubular cells in vivo and in vitro. These data indicated that the tight interactions between mitochondria and the ER are compromised in renal tubular cells in the diabetic state, leading to apoptosis and cellular injury. However, previous studies showed that an increase in calcium ions in mitochondria (which requires organelle interaction) can result in calcium overload, leading to apoptosis [43], which seems to be contrary to our results. However, previously study has also reported that increasing the concentration of calcium in the mitochondria can boost the metabolism of mitochondria to enhance the adaptability of cells to stressful situations [44]. At the same time, another group has demonstrated that increasing mitochondrial ER coupling can promote mitochondrial respiration and biological energy, thereby relieving ER stress [37]. Thus, we believe that the reduction of MAM integrity in diabetic kidneys can cause apoptosis in DN.

DsbA-L has been demonstrated to possess peroxidase activity towards tert-butyl hydroperoxide, cumene hydroperoxide, and 15-S-hydroperocy-5, 8, 11, 13-eicosatetraenoic acid, and it also plays an important role in the detoxification of lipid peroxides [45]. In addition to detoxification properties, this protein exhibits a multitude of varying actions. Intriguingly, overexpression of DsbA-L led to resistance to diet-induced obesity and insulin resistance possibly via adiponectin-dependent mechanisms [46]. However, DsbA-L has been shown to play a critical role in inhibiting ER stress to maintain normal cellular homeostasis [47]. In addition, a recent mass spectrometric study demonstrated that DsbA-L may function as a mimic of the functionality of MAM proteins [17]. Along these lines, we noted in the current study that the expression of DsbA-L in MAM was downregulated in the kidneys of DN mice and in HK-2 cells under HG conditions, and this downregulation was accompanied by increased apoptosis. In addition, the disrupted MAM integrity was further accentuated in the kidneys of diabetic DsbA-L$^{-/-}$ mice compared with that in diabetic mice. However, the mitochondrial morphology and MAM integrity of the DsbA-L$^{-/-}$ in the absence of diabetes had no obvious changes, which are similar to those reported by others, compared to those of the wild type group [16]. The reasons for this phenomenon may be that DsbA-L plays a mitochondrial protective role under HG-induced stress. Since the activities of phospholipid biosynthetic enzymes in MAMs could represent MAM function [7,23,49], we detected the activities of phospholipid biosynthetic enzymes in MAMs from the kidneys of various groups; a significant decline in the MAM fraction of diabetic mice was found compared to that of the control, and it was further aggravated in the kidneys of diabetic mice with DsbA-L gene deficiency. More importantly, overexpression of DsbA-L in HK-2 cells restored the HG-induced dysfunction of MAM and reduced apoptosis. The mechanisms involved in this phenomenon with regard to MAM dysfunction were investigated with the overexpression of FATE-1.

FATE1 is a cancer testis antigen that can dissociate the ER-mitochondrial connection [10]. To verify whether DsbA-L negates apoptosis by maintaining MAM integrity, we cotransfected the FATE1 plasmid into HK-2 cells, followed by exposure to ambient HG. We noted that overexpression of FATE-1 in HK-2 cells inhibited DsbA-L-mediated MAM integrity and the antiapoptotic effects in HG. In addition, to determine whether disrupting MAMs in HK-2 cells was sufficient to promote cell apoptosis, we treated HK-2 cells with HG, and a notable disruption of MAM integrity was observed, accompanied by an obvious increase in the expression of cleaved caspase-3 compared to that of the LG treatment, while further aggravation was observed with overexpression of FATE-1 (data not shown). These results suggest that maintaining MAM integrity in HK-2 cells plays an important role in preventing apoptosis induced by HG. These results indicated that DsbA-L exerted its antiapoptotic effect by maintaining the association between mitochondria and the ER. In terms of MAM integrity, one of the mitochondrial proteins is MFN-2, a member of the mitofusin family that is localized in the MAM [50] and participates in regulating mitochondrial dynamic changes, ER morphology and function [30]. MFN-2 expression was reduced in obese and diabetic patients [51,52]. Gene disruption of MFN-2 uncouples the ER-mitochondrial interaction [53,54] and thus causes dysfunction in mitochondrial homeostasis [55]. To understand the mechanisms by which DsbA-L regulates MAM integrity via MFN-2, we evaluated the expression of MFN-2 using in vivo and in vitro model systems. We observed that the expression of MFN-2 was downregulated in the kidneys of DN mice and was further reduced in diabetic DsbA-L$^{-/-}$ mice. Treatment of HK-2 cells with HG also inhibited the expression of MFN-2, but the effect was partially blocked by the overexpression of DsbA-L. Given the above observations, we speculated that glutathione S-transferase (GST)-kappa1 (GSTK-1), another name for DsbA-L, potentially regulates the integrity of the MAM though the DsbA-L/MFN-2 pathway. However, further studies are needed to delineate the precise molecular mechanism(s) by which MAM integrity is disrupted in HG conditions.

In summary, we demonstrated that disruption of the ER-mitochondrial interaction is closely associated with the downregulation of DsbA-L expression and subsequent increased apoptosis in the kidneys of diabetic patients and mice. Furthermore, gene disruption of DsbA-L adversely affects MAM integrity, which is accompanied by increased apoptosis in tubular cells. Second, the mechanism by which DsbA-L ameliorates renal injury may be mediated by inhibiting apoptosis while maintaining MAM integrity and MFN-2 expression. These studies should help elucidate the precise mechanism(s) by which DsbA-L regulates MAM integrity using a conditional knockout of DsbA-L with directed selected expression in the renal proximal tubular cells. Finally, the presented data should also provide momentum to investigate agonists of the MAM and DsbA-L as potential therapeutic agents to inhibit the progression of DN.

Conflicts of interest statement

Acknowledgments

Author contributions

M.Y., L.Z., P.G., X.J.Z., Y.C.H., X.H.C., C.R.L, and L.L. designed and performed the experiments and analysed the data; Y.X., L.W. and L.X. conceived the project, S.G.Y., F.Y.L. and L.Q.D. supervised the work, and Y.S.K. and L.S. wrote the manuscript.

References

[1] Krolewski AS, Skupien J, Rossing P, Warram JH. Fast renal decline to end-stage renal disease: an unrecognized feature of nephropathy in diabetes. Kidney Int 2017;91: 1300–11.

[2] Nakatsuka A, Wada J, Makino H. Cell cycle abnormality in metabolic syndrome and nuclear receptors as an emerging therapeutic target. Acta Med Okayama 2013;67: 129–34.

[3] Balasescu E, Ion DA, Cioplea M, Zurac S. Caspases, cell death and diabetic nephropathy. Rom J Intern Med 2015;53:296–303.

[4] Wang FY, Tang XM, Wang X, Huang KB, Feng HW, Chen ZF, et al. Mitochondria-targeted platinum(II) complexes induce apoptosis-dependent autophagic cell death mediated by ER-stress in A549 cancer cells. Eur J Med Chem 2018;155: 639–50.

[5] van Vliet AR, Agostinis P. Mitochondria-associated membranes and ER stress. Curr Top Microbiol Immunol 2018;414:73–102.

[6] Gomez-Suaga P, Paillusson S, Miller C. ER-mitochondria signaling regulates autophagy. Autophagy 2017;13:1250–1.

[7] Vance JE. MAM (mitochondria-associated membranes) in mammalian cells: lipids and beyond. Biochim Biophys Acta 2014;1841:595–609.

[8] Doghman-Bouguerra M, Granatiero V, Sbiera S, Sbiera I, Lacas-Gervais S, Brau F, et al. FATE1 antagonizes calcium- and drug-induced apoptosis by uncoupling ER and mitochondria. EMBO Rep 2016;17:1264–80.

[9] Bui M, Gilady SY, Fitzsimmons RE, Benson MD, Lynes EM, Gesson K, et al. Rab32 modulates apoptosis onset and mitochondria-associated membrane (MAM) properties. J Biol Chem 2010;285:31590–602.

[10] Tubbs E, Chanon S, Robert M, Bendridi N, Bidaux G, Chauvin MA, et al. Disruption of mitochondria-associated endoplasmic reticulum membrane (MAM) integrity contributes to muscle insulin resistance in mice and humans. Diabetes 2018;67:636–50.

[11] Thivolet C, Vial G, Cassel R, Rieusset J, Madec AM. Reduction of endoplasmic reticulum- mitochondria interactions in beta cells from patients with type 2 diabetes. Plos One 2017;12:e182027.

[12] Gelmetti V, De Rosa P, Torosantucci L, Marini ES, Romagnoli A, Di Rienzo M, et al. PINK1 and BECN1 relocalize at mitochondria-associated membranes during mitophagy and promote ER-mitochondria tethering and autophagosome formation. Autophagy 2017;13:654–69.

[13] Harris JM, Meyer DJ, Coles B, Ketterer B. A novel glutathione transferase (13–13) isolated from the matrix of rat liver mitochondria having structural similarity to class theta enzymes. Biochem J 1991;278(Pt 1):137–41.

[14] Zhou L, Liu M, Zhang J, Chen H, Dong LQ, Liu F. DsbA-L alleviates endoplasmic reticulum stress-induced adiponectin downregulation. Diabetes 2010;59:2809–16.

[15] Sasagawa S, Nishimura Y, Okabe S, Murakami S, Ashikawa Y, Yuge M, et al. Down-regulation of GSTK1 is a common mechanism underlying hypertrophic cardiomyopathy. Front Pharmacol 2016;7:162.

[16] Blackburn AC, Coggan M, Shield AJ, Cappello J, Theodoratos A, Murray TP, et al. Glutathione transferase kappa deficiency causes glomerular nephropathy without overt oxidative stress. Lab Invest 2011;91:1572–83.

[17] Sala-Vila A, Navarro-Lerida I, Sanchez-Alvarez M, Bosch M, Calvo C, Lopez JA, et al. Interplay between hepatic mitochondria-associated membranes, lipid metabolism and caveolin-1 in mice. Sci Rep 2016;6:27351.

[18] Chen GT, Yang M, Chen BB, Song Y, Zhang W, Zhang Y. 2,3,5,4'-Tetrahydroxystilbene-2-O-beta-d-glucoside exerted protective effects on diabetic nephropathy in mice with hyperglycemia induced by streptozotocin. Food Funct 2016;7:4628–36.

[20] Tubbs E, Theurey P, Vial G, Bendridi N, Bravard A, Chauvin MA, et al. Mitochondria-associated endoplasmic reticulum membrane (MAM) integrity is required for insulin signaling and is implicated in hepatic insulin resistance. Diabetes 2014;63: 3279–94.

[21] Xiao L, Zhu X, Yang S, Liu F, Zhou Z, Zhan M, et al. Rap1 ameliorates renal tubular injury in diabetic nephropathy. Diabetes 2014;63:1366–80.

[22] Horner SM, Wilkins C, Badil S, Iskarpatyoti J, Gale MJ. Proteomic analysis of mitochondrial-associated ER membranes (MAM) during RNA virus infection reveals dynamic changes in protein and organelle trafficking. Plos One 2015;10:e117963.

[23] Vance JE, Stone SJ, Faust JR. Abnormalities in mitochondria-associated membranes and phospholipid biosynthetic enzymes in the mnd/mnd mouse model of neuronal ceroid lipofuscinosis. Biochim Biophys Acta 1997;1344:286–99.

[24] Liu M, Zhou L, Xu A, Lam KS, Wetzel MD, Xiang R, et al. A disulfide-bond A oxidoreductase-like protein (DsbA-L) regulates adiponectin multimerization. Proc Natl Acad Sci U S A 2008;105:18302–7.

[25] Sawai H, Domae N. Discrimination between primary necrosis and apoptosis by necrostatin-1 in Annexin V-positive/propidium iodide-negative cells. Biochem Biophys Res Commun 2011;411:569–73.

[26] Yang S, Zhao L, Han Y, Liu Y, Chen C, Zhan M, et al. Probucol ameliorates renal injury in diabetic nephropathy by inhibiting the expression of the redox enzyme p66Shc. Redox Biol 2017;13:482–97.

[27] Chen X, Han Y, Gao P, Yang M, Xiao L, Xiong X, et al. Disulfide-bond A oxidoreductase-like protein protects against ectopic fat deposition and lipid-related kidney damage in diabetic nephropathy. Kidney Int Apr 2019;95(4):880–95.

[28] Han Y, Xu X, Tang C, Gao P, Chen X, Xiong X, et al. Reactive oxygen species promote tubular injury in diabetic nephropathy: the role of the mitochondrial ros-txnip-nlrp3 biological axis. Redox Biol 2018;16:32–46.

[29] Ma JH, Shen S, Wang JJ, He Z, Poon A, Li J, et al. Comparative proteomic analysis of the mitochondria-associated ER membrane (MAM) in a long-term type 2 diabetic rodent model. Sci Rep-UK 2017;7.

[30] de Brito OM, Scorrano L. Mitofusin 2 tethers endoplasmic reticulum to mitochondria. Nature 2008;456:605–10.

[31] Jiang L, Chen C, Yuan T, Qin Y, Hu M, Li X, et al. Clinical severity of Gitelman syndrome determined by serum magnesium. Am J Nephrol 2014;39:357–66.

[33] Sifuentes-Franco S, Padilla-Tejeda DE, Carrillo-Ibarra S, Miranda-Diaz AG. Oxidative stress, apoptosis, and mitochondrial function in diabetic nephropathy. Int J Endocrinol 2018;2018:1875870.

[34] Bravo-Sagua R, Torrealba N, Paredes F, Morales PE, Pennanen C, Lopez-Crisosto C, et al. Organelle communication: signaling crossroads between homeostasis and disease. Int J Biochem Cell Biol 2014;50:55–9.

[35] Giacomello M, Pellegrini L. The coming of age of the mitochondria-ER contact: a matter of thickness. Cell Death Differ 2016;23:1417–27.

[37] Bravo R, Vicencio JM, Parra V, Troncoso R, Munoz JP, Bui M, et al. Increased ER-mitochondrial coupling promotes mitochondrial respiration and bioenergetics during early phases of ER stress. J Cell Sci 2011;124:2143–52.

[38] Theurey P, Tubbs E, Vial G, Jacquemetton J, Bendridi N, Chauvin MA, et al. Mitochondria-associated endoplasmic reticulum membranes allow adaptation of mitochondrial metabolism to glucose availability in the liver. J Mol Cell Biol 2016; 8:129–43.

[39] Arruda AP, Pers BM, Parlakgul G, Guney E, Inouye K, Hotamisligil GS. Chronic enrichment of hepatic endoplasmic reticulum-mitochondria contact leads to mitochondrial dysfunction in obesity. Nat Med 2014;20:1427–35.

[42] Tubbs E, Rieusset J. Study of endoplasmic reticulum and mitochondria interactions by in situ proximity ligation assay in fixed cells. J Vis Exp Dec 10 2016;118.

[43] Giorgi C, Bonora M, Sorrentino G, Missiroli S, Poletti F, Suski JM, et al. p53 at the endoplasmic reticulum regulates apoptosis in a Ca2+−dependent manner. Proc Natl Acad Sci U S A 2015;112:1779–84.

[44] Green DR, Wang R. Calcium and energy: making the cake and eating it too? Cell 2010;142:200–2.

[45] Morel F, Rauch C, Petit E, Piton A, Theret N, Coles B, et al. Gene and protein characterization of the human glutathione S-transferase kappa and evidence for a peroxisomal localization. J Biol Chem 2004;279:16246–53.

[46] Liu M, Xiang R, Wilk SA, Zhang N, Sloane LB, Azarnoush K, et al. Fat-specific DsbA-L overexpression promotes adiponectin multimerization and protects mice from diet-induced obesity and insulin resistance. Diabetes 2012;61:2776–86.

[47] Liu M, Chen H, Wei L, Hu D, Dong K, Jia W, et al. Endoplasmic reticulum (ER) localization is critical for DsbA-L protein to suppress ER stress and adiponectin downregulation in adipocytes. J Biol Chem 2015;290:10143–9.

[49] Area-Gomez E. Assessing the function of mitochondria-associated ER membranes. Methods Enzymol 2014;547:181–97.

[50] Papanicolaou KN, Khairallah RJ, Ngoh GA, Chikando A, Luptak I, O'Shea KM, et al. Mitofusin-2 maintains mitochondrial structure and contributes to stress-induced permeability transition in cardiac myocytes. Mol Cell Biol 2011;31:1309–28.

[51] Bach D, Naon D, Pich S, Soriano FX, Vega N, Rieusset J, et al. Expression of Mfn2, the Charcot-Marie-Tooth neuropathy type 2A gene, in human skeletal muscle: effects of type 2 diabetes, obesity, weight loss, and the regulatory role of tumor necrosis factor alpha and interleukin-6. Diabetes 2005;54:2685–93.

[52] Hernandez-Alvarez MI, Thabit H, Burns N, Shah S, Brema I, Hatunic M, et al. Subjects with early-onset type 2 diabetes show defective activation of the skeletal muscle PGC-1{alpha}/Mitofusin-2 regulatory pathway in response to physical activity. Diabetes Care 2010;33:645–51.

[53] de Brito OM, Scorrano L. Mitofusin-2 regulates mitochondrial and endoplasmic reticulum morphology and tethering: the role of Ras. Mitochondrion 2009;9:222–6.

[54] Naon D, Zaninello M, Giacomello M, Varanita T, Grespi F, Lakshminarayan S, et al. Critical reappraisal confirms that Mitofusin 2 is an endoplasmic reticulum-mitochondria tether. Proc Natl Acad Sci U S A 2016;113:11249–54.

[55] Chen Y, Csordas G, Jowdy C, Schneider TG, Csordas N, Wang W, et al. Mitofusin 2-containing mitochondrial-reticular microdomains direct rapid cardiomyocyte bioenergetic responses via interorganelle Ca(2+) crosstalk. Circ Res 2012;111:863–75.